Inorganic Chemistry

Article

pubs.acs.org/IC

# FTIR Study of Manganese Dimers with Carboxylate Donors As Model Complexes for the Water Oxidation Complex in Photosystem II

Gustav Berggren,[†] Magnus F. Anderlund, Stenbjörn Styring, and Anders Thapper*

Department of Photochemistry and Molecular Science, Uppsala University, P.O. Box 523, S-75120 Uppsala, Sweden

Supporting Information

**ABSTRACT:** The carboxylate stretching frequencies of two high-valent, di-$\mu$-oxido bridged, manganese dimers has been studied with IR spectroscopy in three different oxidation states. Both complexes contain one monodentate carboxylate donor to each Mn ion, in one complex, the carboxylate is coordinated perpendicular to the Mn-($\mu$-O)$_2$-Mn plane, and in the other complex, the carboxylate is coordinated in the Mn-($\mu$-O)$_2$-Mn plane. For both complexes, the difference between the asymmetric and the symmetric carboxylate stretching frequencies decrease for both the $Mn_2^{IV,IV}$ to $Mn_2^{III,IV}$ transition and the $Mn_2^{III,IV}$ to $Mn_2^{III,III}$ transition, with only minor differences observed between the two arrangements of the carboxylate ligand versus the Mn-($\mu$-O)$_2$-Mn plane. The IR spectra also show that both carboxylate ligands are affected for each one electron reduction, i.e., the stretching frequency of the carboxylate coordinated to the Mn ion that is not reduced also shifts. These results are discussed in relation to FTIR studies of changes in carboxylate stretching frequencies in a one electron oxidation step of the water oxidation complex in Photosystem II.

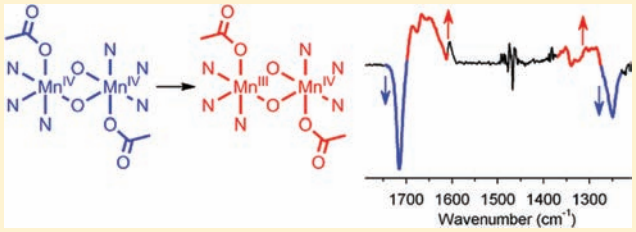


## INTRODUCTION

Carboxylate donors are a reoccurring theme in the active site of many metalloproteins including a number of manganese containing redox active enzymes, e.g., the water oxidation complex (WOC) in Photosystem II (PSII),[1] super oxide dismutase,[2] and manganese catalases.[3] A large number of synthetic manganese complexes incorporating carboxylate ligands, aiming at mimicking functional or spectroscopical aspects of these enzymes, have been reported.[4] The carboxylate group has characteristic IR stretching frequencies that can be used to deduce the coordination mode to metal ions as well as serve as a probe during catalytic turnover.

In PSII, the WOC cycles through five intermediary states (S-states), and each step is accompanied by an electron transfer from the WOC, either alone ($S_1 \rightarrow S_2$) or together with a proton transfer ($S_0 \rightarrow S_1$, $S_2 \rightarrow S_3$).[5] The $S_0 \rightarrow S_1$ and $S_1 \rightarrow S_2$ oxidations are considered to be metal based, while for $S_2 \rightarrow S_3$, both metal based and ligand based oxidations has been proposed. With the recently reported 1.9 Å resolution crystal structure of PSII,[6] the efforts to establish a mechanism for water oxidation in PSII has taken a large step forward. However, even if there is now a good model for the structure of the dark stable $S_1$ state, X-ray crystallography gives limited mechanistic information. Instead, spectroscopic measurements are required to determine what changes the WOC undergoes for each step in the S-cycle. Many spectroscopic techniques have long been employed; the most important being EPR, IR, and X-ray spectroscopy. IR spectroscopy is particularly useful to obtain more specific information on the ligand environment and changes therein, for example, by studying the carboxylate stretching frequencies. FTIR spectroscopy has been used to analyze effects of mutations in the vicinity of the WOC and to follow changes during the S-cycle. To interpret the FTIR data from S-state turnover measurements in PSII, it is crucial to have access to relevant IR data from model complexes. Unfortunately, there are only a few manganese complexes that have been well characterized in multiple oxidation states with regard to carboxylate stretching frequencies.[7−9]

This study aims to provide more data on how the stretching frequencies of monodentally coordinated carboxylates on Mn ions are influenced by the oxidation state of the metal. The study also addresses the influence of the position of the carboxylate in the coordination sphere of the Mn ion. This has been proposed to have a major effect on IR frequencies of carboxylate donors in the WOC during the S-cycle.[10]

We have measured midrange FTIR data for two, crystallographically characterized, high-valent dinuclear Mn complexes (Figure 1), $\mathbf{1}^{2+}$ = $[\mathbf{L1}Mn^{IV}(\mu\text{-}O)_2Mn^{IV}\mathbf{L1}]^{2+}$ (H**L1** = 2-(((2-(bis(pyridin-2-ylmethyl))amino)ethyl)(methyl)amino)acetic acid)[11] and $\mathbf{2}^{+}$ = $[\mathbf{L2}Mn^{III}(\mu\text{-}O)_2Mn^{IV}\mathbf{L2}]^{+}$ (H**L2** = *N*,*N*-bis(2-pyridylmethyl)glycine).[12] The two complexes have almost identical coordination environments. There is, however, a key difference in how the monodentate carboxylate ligands coordinate relative to the Mn-($\mu$-O)$_2$-Mn plane. In complex $\mathbf{1}^{2+}$, the carboxylate coordinates in an axial mode with regards to the Mn-($\mu$-O)$_2$-Mn plane, while in $\mathbf{2}^{+}$ it is coordinating in an equatorial position, trans to a $\mu$-oxido ligand.

Herein, we report changes in the asymmetric ($\nu_a$(COO)) and symmetric ($\nu_s$(COO)) carboxylate stretching frequencies

**Received:** October 27, 2011
**Published:** January 25, 2012

   dx.doi.org/10.1021/ic202323b | *Inorg. Chem.* 2012, 51, 2332−2337

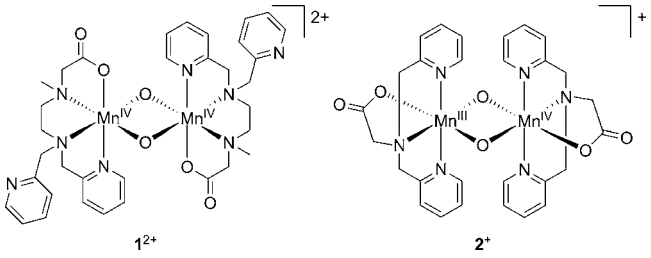


**Figure 1.** Complexes employed in this study.

associated with oxidation state changes in **1** and **2** in solution for the $Mn_2^{IV,IV}$ to $Mn_2^{III,IV}$ transition as well as the $Mn_2^{III,IV}$ to $Mn_2^{III,III}$ transition. The carboxylate stretching frequencies are unambiguously identified using the corresponding $^{13}$C-labeled complexes, **1*** and **2***.

The results from the model complexes are compared with the FTIR spectroscopic data from PSII, focusing on the $S_1 \rightarrow S_2$ transition in the S-cycle of the WOC, which is a one electron oxidation step without any additional proton release from the WOC.[5]

## EXPERIMENTAL SECTION

**Materials.** Reagents were purchased commercially and used as received. Na**L1**,[13] **L2**,[12] and $[\mathbf{L1}Mn^{IV}(\mu\text{-}O)_2Mn^{IV}\mathbf{L1}](ClO_4)_2$ $\{\mathbf{1}(ClO_4)_2\}$[11] were prepared in accordance to the literature, while $[\mathbf{L2}Mn^{III}(\mu\text{-}O)_2Mn^{IV}\mathbf{L2}](PF_6)$ (**2**$PF_6$) was synthesized via a modification of the literature procedure for **2**$ClO_4$[12] where $KPF_6$ was used instead of $NH_4ClO_4$ for precipitation of the product. The isotopologous $^{13}$C-labeled complexes, **1***$(ClO_4)_2$ and **2***$PF_6$, were synthesized by replacing ethyl bromoacetate with ethyl bromoacetate-1-$^{13}$C (99 atom % $^{13}$C). The incorporation of a $^{13}$C-labeled carbonyl carbon was verified by ESI-MS and $^{13}$C NMR.

**Electrochemistry.** Cyclic voltammetry and controlled potential electrolysis were carried out by using an Autolab potentiostat with a GPES electrochemical interface (Eco Chemie). Sample solutions (4 mL) were prepared from dry acetonitrile containing 0.1 M tetrabutylammonium hexaflourophosphate ($TBAPF_6$) (electrochemical grade) as the supporting electrolyte. For cyclic voltammetry, the working electrode was a glassy carbon disk (diameter 3 mm). All cyclic voltammograms shown were recorded at a scan rate of 0.1 V $s^{-1}$. A glassy carbon rod served as the counter electrode, and the reference electrode was a $Ag/Ag^+$ electrode (a silver wire immersed into 10 mM $AgNO_3$ in MeCN) with a potential of −0.07 V vs the ferrocene/ferrocenium ($Fc/Fc^+$) couple in dry MeCN. The counter and reference electrode were in compartments separated from the bulk solution by fritted disks and were the same for both analytical and bulk electrochemical experiments. Before all measurements, oxygen was purged from the stirred solutions using solvent-saturated argon. Samples were kept under argon during the measurements. To obtain EPR spectra of the complexes in different oxidation states, solutions prepared in the same way as described above for analytical electrochemistry, but cooled to −10 °C, were subjected to bulk electrolysis at controlled potentials. A cylindrical platinum grid (4 $cm^2$) was used as the working electrode for bulk electrolysis. The preparative electrolysis experiments were monitored by amperometry and coulometry and took 3−5 min for completion. After electrolysis, aliquots of 100 $\mu$L were taken from the solution, with an airtight, argon-filled syringe, transferred to argon-flushed EPR tubes, frozen, and stored in liquid nitrogen.

**IR Spectroscopy.** IR absorption spectra were recorded in absorbance mode between 4000 and 1000 $cm^{-1}$ for absolute spectra and between 2000 and 1000 $cm^{-1}$ for difference spectra at a resolution of 4 $cm^{-1}$ on a Bruker FTIR spectrometer with the sample as a solution in a custom built liquid sample spectroelectrochemical cell between $CaF_2$ windows and a path length of 1 mm.

The solutions were prepared in $CD_3CN$ (99.8 atom % D) dried over molecular sieves. The use of deuterated solvent minimized the background absorption in the range of the carboxylate bands (1800−1200 $cm^{-1}$). Minor differences in residual $H_2O$ content between sample and background measurement gave rise to incomplete background correction in some spectra. Where necessary, the remaining absorption band of $H_2O$ (1632 $cm^{-1}$, $\nu_{(H-O-H)}$) was subtracted from the presented spectra. Different oxidation states of the complexes were prepared by preparative bulk electrolysis as described above but using $CD_3CN$ as solvent. Alternatively, $\mathbf{1}^+$ could be prepared by chemical reduction of $\mathbf{1}^{2+}$ in $CD_3CN$ using 1 equivalent of ferrocene. Electrochemically induced difference IR measurements were performed on 2 mM solutions of complexes **1** and **2** and 1 mM solutions for **1*** and **2*** in $CD_3CN$ with 0.1 M $TBAPF_6$. The difference IR spectra were recorded in the custom built cell using a Pt-grid as the working electrode and a Pt-rod as the counter electrode. The reference electrode was of the same type as described for electrochemistry, but using $CD_3CN$, and connected to the cell via a salt bridge. For the difference spectra presented in this work, a background spectrum was collected in the higher oxidation state, and spectra were recorded every five seconds during continuous electrochemical reduction (unless otherwise stated). The final spectrum in the series was used as the difference spectrum for the oxidized-to-reduced transition and is equivalent to a reduced state-minus-oxidized state spectrum.

## RESULTS

Complex **1**$(ClO_4)_2$ was prepared as reported previously,[11] and **2**$PF_6$ was prepared using a modified literature procedure.[12] Additionally, their isotopologues (**1***$(ClO_4)_2$ and **2***$PF_6$), incorporating $^{13}$C-labeled carbonyl carbons, were prepared using the same synthesis pathway.

Electrochemical measurements were performed in $CH_3CN$. The complexes had similar CV-traces, displaying two quasi-reversible processes (Figure S1 in the Supporting Information). These were assigned to $Mn_2$(IV,IV)/(III,IV) and $Mn_2$(III,IV)/

**Scheme 1. Oxidation/Reduction Steps and Oxidation States of the Complexes Involved in This Study**[a]

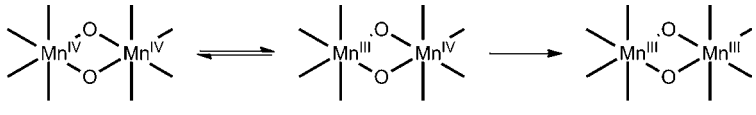


| | | | |
|---|---|---|---|
| Absolute spectra | $\mathbf{1}^{2+}$ (2a')<br>$\mathbf{2}^{2+}$ (2a'') | $\mathbf{1}^{+}$ (2c')<br>$\mathbf{2}^{+}$ (2c'') | $\mathbf{1}^{0}$ n/a<br>$\mathbf{2}^{0}$ n/a |
| Difference spectra | $\mathbf{1}^{2+} \rightarrow \mathbf{1}^{+}$ (2b')<br>$\mathbf{2}^{2+} \rightarrow \mathbf{2}^{+}$ (2b'') | $\mathbf{1}^{+} \rightarrow \mathbf{1}^{0}$ (2d')<br>$\mathbf{2}^{+} \rightarrow \mathbf{2}^{0}$ (2d'') | |

[a]Numbers in parentheses refer to spectra in Figure 2; n/a = not available.


dx.doi.org/10.1021/ic202323b | Inorg. Chem. 2012, 51, 2332−2337

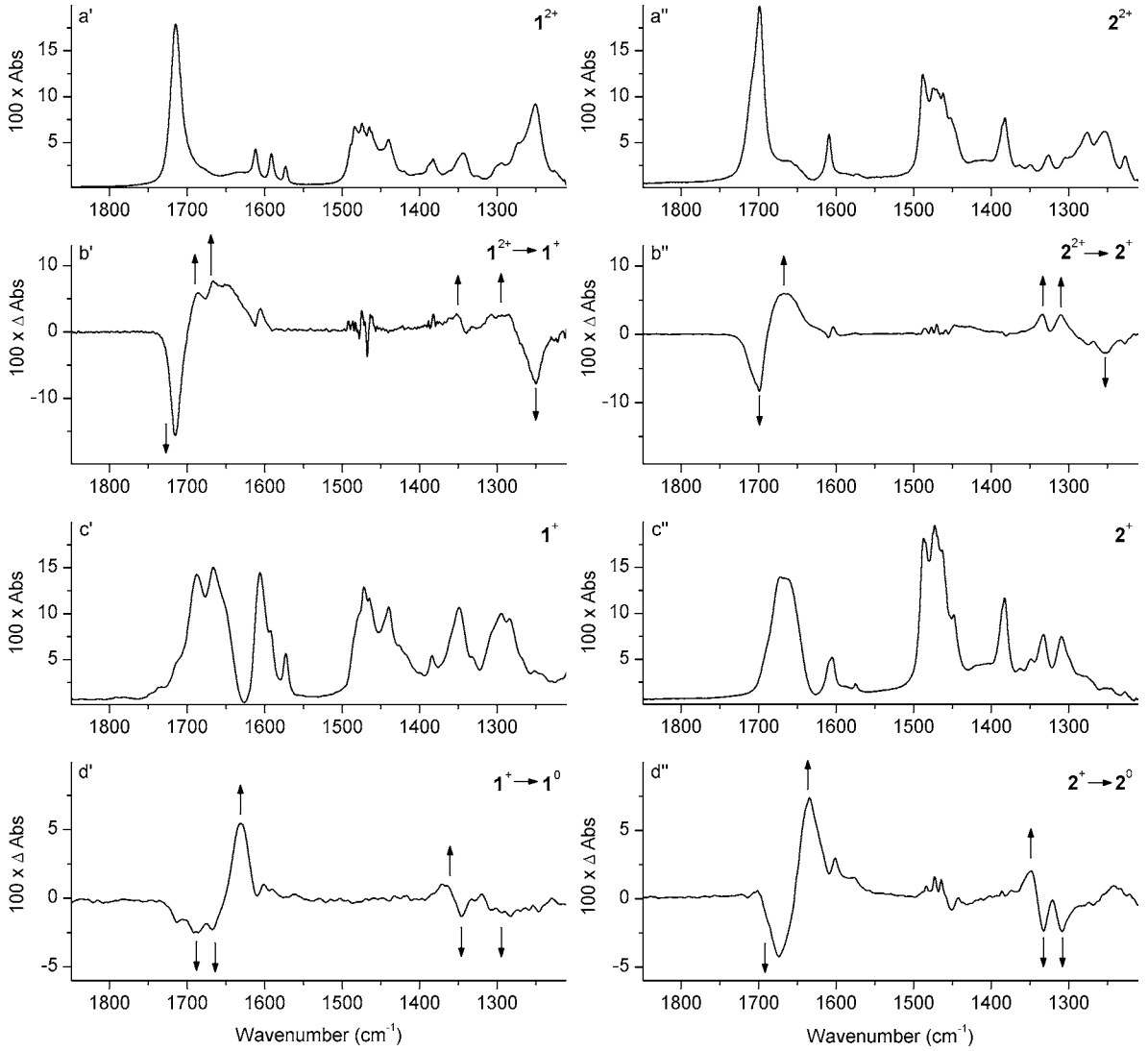


**Figure 2.** Absolute (a and c) and difference (b and d) IR spectra of **1** (2 mM) and **2** (2 mM), left and right panels, respectively. The arrows in the difference spectra (b and d) indicate appearance of peaks/troughs. (a) Absolute spectra of the $Mn_2^{IV,IV}$ state. The absolute spectrum of $\mathbf{2}^{2+}$ (a″) was obtained by bulk electrolysis of $\mathbf{2}^{+}$ at 0.85 V. (b) Difference spectra of the $Mn_2^{IV,IV} \rightarrow Mn_2^{III,IV}$ transitions ($Mn_2^{III,IV}$-minus-$Mn_2^{IV,IV}$) from reduction of the $Mn_2^{IV,IV}$ state at 0.05 V. (c) Absolute spectrum of the $Mn_2^{III,IV}$ state. The spectrum of $\mathbf{1}^{+}$ (c′) was obtained by chemical reduction using 1 equiv of ferrocene. (d) Difference spectra of the $Mn_2^{III,IV} \rightarrow Mn_2^{III,III}$ transitions ($Mn_2^{III,III}$-minus-$Mn_2^{III,IV}$) from reduction of the $Mn_2^{III,IV}$ state at −0.67 V. Because of the instability of the $Mn_2^{III,III}$ state, the spectra were collected before the reduction was complete. All spectra were obtained in $CD_3CN$.

(III,III) redox couples, respectively, in line with previous studies.[11,14] Complexes **1** and **2** were stable on at least a minute time scale in both their $Mn_2^{IV,IV}$ and $Mn_2^{III,IV}$ oxidation states. Conversely, the $Mn_2^{III,III}$ complexes were found to be unstable on this time scale, and only difference spectra for the $Mn_2^{III,IV}$ to $Mn_2^{III,III}$ reduction could be obtained.

The FTIR data was recorded in $CD_3CN$ solutions using either standard absolute spectra or electrochemically induced difference spectra. For bulk electrolysis, potentials of 0.85, 0.05, or −0.67 V were used to obtain the $Mn_2^{IV,IV}$ ($\mathbf{1}^{2+}$ and $\mathbf{2}^{2+}$), $Mn_2^{III,IV}$ ($\mathbf{1}^{+}$ and $\mathbf{2}^{+}$), or $Mn_2^{III,III}$ ($\mathbf{1}^{0}$ and $\mathbf{2}^{0}$) form of the complexes, respectively. The different oxidation states and transitions between them are shown in Scheme 1.

The absolute spectra of $\mathbf{1}^{2+}$ and $\mathbf{2}^{+}$ (i.e., the oxidation states of the solid starting materials) in $CD_3CN$ are shown in Figure 2a′ and c″, respectively, and in Figure S2, Supporting Information. Both complexes show strong signals attributable to stretches of the carboxylate ligands (see below). We will refer to them as $\nu_a$(COO) for stretches in the high field region and $\nu_s$(COO) for stretches in the low field region, even if the bands might have some $\nu$(C═O) and $\nu$(C−O) character, respectively (especially in the $Mn_2^{IV,IV}$ state).[15] There are some differences between the solution spectra and the corresponding spectra of $\mathbf{1}(ClO_4)_2$ and $\mathbf{2}PF_6$ measured in KBr pellets (Figure S2, Supporting Information). Both KBr spectra appear to have contributions from two different species, one of the species in each spectrum has IR stretches very similar to the corresponding complex in solution. An EPR spectrum of a frozen solution of $\mathbf{1}(ClO_4)_2$ confirms the $Mn_2^{IV,IV}$ oxidation state (~5% $Mn_2^{III,IV}$) and an EPR spectrum of $\mathbf{2}PF_6$ shows the complex in the $Mn_2^{III,IV}$ oxidation state in agreement with the literature.[11,12] Therefore, the second species in the KBr IR spectra cannot be a different oxidation state for either of the complexes. Instead, the differences are likely to be attributable to effects arising from, for example, crystal packing and differences in H-bonding in the solvent versus solid state.

The difference IR spectrum of the $\mathbf{1}^{2+} \rightarrow \mathbf{1}^{+}$ reduction (equivalent to a $\mathbf{1}^{+}$-minus-$\mathbf{1}^{2+}$ spectrum) is shown in Figure 2b′.


dx.doi.org/10.1021/ic202323b | Inorg. Chem. 2012, 51, 2332−2337

**Table 1. Changes in Carboxylate Stretching Frequencies upon Reduction of Complex 1 and Complex 2[a]**

| | complex 1 | | | complex 2 | | |
|---|---|---|---|---|---|---|
| stretch | trough | peak | shift[b] | trough | peak | shift[b] |
| IV,IV to III,IV | | | | | | |
| $\nu_a$(COO) ($cm^{-1}$) | 1714 | 1688; 1667 | −26; −47 | 1699 | 1675; (1655) | −24; (−44) |
| $\nu_s$(COO) ($cm^{-1}$) | 1251 | 1295; 1348 | 44; 97 | 1255; 1275 | 1309; (1332) | 54; (77) |
| III,IV to III,III | | | | | | |
| $\nu_a$(COO) ($cm^{-1}$) | 1688; 1667 | 1631 | −36; −57 | 1675; (1655) | 1631 | (−24); −44 |
| $\nu_s$(COO) ($cm^{-1}$) | 1295; 1348 | 1370 | 22; 75 | 1309; (1332) | 1348 | (16); 39 |

[a]From the IR difference spectra in Figure 2. [b]Difference between the trough(s) and the peak(s).

In the $\nu_a$(COO) stretching region, there is a trough at 1714 $cm^{-1}$ and two peaks at 1688 and 1667 $cm^{-1}$. In the $\nu_s$(COO) region, there is a trough at 1251 $cm^{-1}$ and broad positive peaks at around 1295 and 1348 $cm^{-1}$ (Table 1).[16] Therefore, all carboxylate bands are affected by the reduction and/or the overall change in charge of the complex, also the bands from the carboxylate that is still coordinated to a Mn(IV) ion. This is also seen in the absolute spectrum of $\mathbf{1}^{+}$ (Figure 2c′) where the peaks from $\mathbf{1}^{2+}$ at 1714 and 1251 $cm^{-1}$ are completely absent.

Based on the difference spectrum for the reduction of the $^{13}$C labeled $\mathbf{1}^{*2+}$ (Figure 3), together with the absolute spectra of

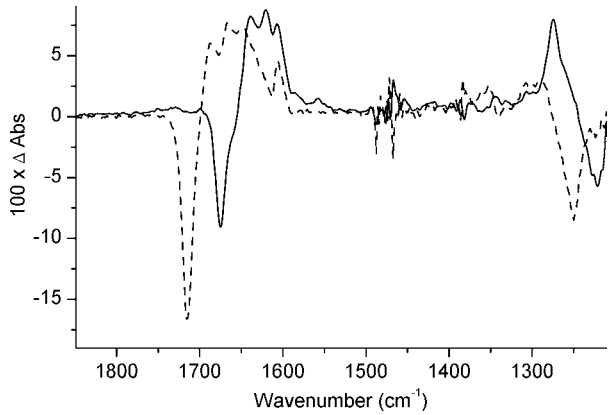


**Figure 3.** Difference spectra for the $\mathbf{1}^{2+} \rightarrow \mathbf{1}^{+}$ (dashed line, 2 mM) and the $\mathbf{1}^{*2+} \rightarrow \mathbf{1}^{*+}$ (full line, 1 mM, multiplied by 2) reductions at 0.05 V.

$\mathbf{1}^{2+}$, $\mathbf{1}^{+}$, $\mathbf{1}^{*2+}$, and $\mathbf{1}^{*+}$ (Figure S3, Supporting Information), these bands are assigned as being related to the carboxylate stretches. There is no shift of the sharp peak at 1606 $cm^{-1}$ in the $^{13}$C labeled spectra, and it is likely associated with a C═C pyridine stretch.[14]

As mentioned above, $\mathbf{1}^{0}$ is not stable on longer time scales, but nevertheless, a difference FTIR spectrum of the $\mathbf{1}^{+} \rightarrow \mathbf{1}^{0}$ transition could be obtained (Figure 2d′) if it was recorded before other species than $\mathbf{1}^{0}$ appeared, meaning before all $\mathbf{1}^{+}$ was reduced. One positive peak at 1631 $cm^{-1}$ in the $\nu_a$(COO) stretching region and one at 1370 $cm^{-1}$ in the $\nu_s$(COO) stretching region are attributed to $\mathbf{1}^{0}$ (Table 1).

Difference spectra of the $\mathbf{2}^{2+} \rightarrow \mathbf{2}^{+}$ transition and the $\mathbf{2}^{+} \rightarrow \mathbf{2}^{0}$ transition are shown in Figure 2b″ and d″, respectively, together with the absolute spectra of $\mathbf{2}^{2+}$ (obtained by bulk electrolysis at 0.85 V, Figure 2a″) and $\mathbf{2}^{+}$ (Figure 2c″). The difference spectrum of the $\mathbf{2}^{2+} \rightarrow \mathbf{2}^{+}$ transition has strong similarities with the difference spectrum of the $\mathbf{1}^{2+} \rightarrow \mathbf{1}^{+}$ transition with a trough at 1699 $cm^{-1}$ and an increase in a broad feature with two unresolved peaks at around 1675 and 1655 $cm^{-1}$. In the $\nu_s$(COO) region, there are troughs at 1275 and 1255 $cm^{-1}$ and two sharp peaks at 1332 and 1309 $cm^{-1}$ (Table 1). The difference spectrum for the $\mathbf{2}^{*+} \rightarrow \mathbf{2}^{*2+}$ oxidation (Figure S4, Supporting Information) confirms the assignment of these bands as originating from carboxylate stretches. The difference spectrum for the $\mathbf{2}^{+} \rightarrow \mathbf{2}^{0}$ reduction resembles the difference spectrum for the $\mathbf{1}^{+} \rightarrow \mathbf{1}^{0}$ reduction with one positive feature at 1631 $cm^{-1}$ in the $\nu_a$(COO) region and one peak (1348 $cm^{-1}$) in the $\nu_s$(COO) region assigned to $\mathbf{2}^{0}$ (Table 1). This spectrum also had to be recorded before all $\mathbf{2}^{+}$ was reduced. Following the development of the difference IR spectra with time for the oxidation of $\mathbf{2}^{+} \rightarrow \mathbf{2}^{2+}$ (Figure S5, Supporting Information, black spectra) or reduction of $\mathbf{2}^{2+} \rightarrow \mathbf{2}^{+}$ (Figure S5, Supporting Information, red spectra), the spectra show clear isosbestic points and no signs of intermediate products. For the corresponding experiment where $\mathbf{2}^{+}$ was reduced to $\mathbf{2}^{0}$ (Figure S6, Supporting Information, black spectra), the appearance of more than one species was observed after a short reduction (~30 s). However, when the process was reversed at the end of the experiment so that $\mathbf{2}^{0}$ was oxidized back to $\mathbf{2}^{+}$ (Figure S6, Supporting Information, red spectra), most of the $\mathbf{2}^{+}$ was recovered, and the major additional peak remaining was found at 1632 $cm^{-1}$, corresponding to the $\nu_{(H-O-H)}$ absorption band from water.

## DISCUSSION

For both complexes **1** and **2**, the decrease in the Δ value (Δ = $\nu_a$(COO) − $\nu_s$(COO)) is large for the $Mn_2^{IV,IV}$ to $Mn_2^{III,IV}$ reduction (70−125 $cm^{-1}$) and slightly smaller for the $Mn_2^{III,IV}$ to $Mn_2^{III,III}$ reduction (60−80 $cm^{-1}$).[18] The shift for each reduction is somewhat larger if the monodentate carboxylates are coordinated perpendicular to the Mn-($\mu$-O)$_2$-Mn plane (as in **1**) than if they are coordinated in the plane (as in **2**), but the differences are not pronounced. There are few reports in the literature of IR stretching frequencies of monodentate carboxylate ligands to high-valent Mn dimers.[9,19,20] In most studies, the $\nu_a$(COO) and $\nu_s$(COO) stretching frequencies are measured in the solid state and are not unambiguously assigned, which make comparisons with our study difficult. The dimeric complex $[Mn_2O_2(pic)_4]^{n-}$ (picH = picolylic acid) was studied in both the $Mn_2^{IV,IV}$ ($n$ = 0) and $Mn_2^{III,IV}$ ($n$ = 1) oxidation states, but the structure was not reported. A decrease in the Δ value (~50 $cm^{-1}$) was observed when the complex was reduced from $Mn_2^{IV,IV}$ to $Mn_2^{III,IV}$.[9] However, later studies[20] have shown that two different coordination geometries could be obtained for the $Mn_2^{IV,IV}$ complex making it problematic to compare the results to this study.

For the complex $[(tacn)Mn(\mu\text{-}O)(\mu\text{-}OAc)_2Mn(tacn)]^{n+}$ (tacn = 1,4,7-trimethyl-l,4,7-triazacylononane) with a bridging carboxylate, the Δ value increased when the complex was reduced from the $Mn_2^{III,IV}$ ($n$ = 3) to the $Mn_2^{III,III}$ state ($n$ = 2),[7]


dx.doi.org/10.1021/ic202323b | Inorg. Chem. 2012, 51, 2332−2337

i.e., the opposite of what we observed for the monodentate carboxylates. For the complex $[Mn_2(bpmp)(\mu\text{-}OAc)_2]^{n+}$ (bpmpH = 2,6-bis[bis(2-pyridylmethyl)-amino]methyl-4-methylphenol) with two bridging carboxylates, the Δ value was almost constant when going from the $Mn_2^{III,III}$ ($n$ = 3) to the $Mn_2^{II,III}$ ($n$ = 2) state.[8] The wavenumber for the $\nu_a$(COO) increases upon reduction for both complexes with bridging carboxylates, whereas the trend is the opposite for $\nu_a$(COO) for the two complexes with monodentate carboxylates in this study.

The crystal structure of $\mathbf{2}^+$ clearly shows that the $Mn_2^{III,IV}$ complex is not a (completely) delocalized system, the $N_{py}$–Mn bonds, perpendicular to the Mn-($\mu$-O)$_2$-Mn plane, are elongated by ∼0.07 Å on the Mn(III) ion compared to the Mn(IV) ion.[12] In the IR spectrum of $\mathbf{1}^+$ and, to a smaller degree, in the IR spectrum of $\mathbf{2}^+$, two bands are present for the $\nu_a$(COO) stretching frequencies, which also indicate a mixed-valence $Mn_2^{III,IV}$ state in solution rather than a delocalized +3.5 oxidation state.

The 1.9 Å resolution crystal structure of PSII shows that the WOC consists of a $CaMn_4O_5$ cluster composed of oxido-bridged metal ions held in the protein cavity by six carboxylate donors and one histidine residue.[6] IR spectroscopical studies of PSII in the different S-states have tried to identify ligands to the WOC,[1] e.g., glutamate and aspartate side chains, and monitor structural changes during the S-cycle. Despite a wealth of data obtained, assigning IR bands to the carboxylate ligands has so far proven difficult.

To explain this discrepancy, it has been argued that a carboxylate donor outside of the Jahn–Teller (JT) axis[21] should experience a much smaller shift between Mn(III) and Mn(IV) compared to a carboxylate donor along the JT axis.[10] The reasoning is that the Mn–O bond length on a Mn(III) ion will change more upon oxidation if the bond is along an elongated axis than if the bond is along a nonelongated axis since no axis will be elongated on a Mn(IV) ion.

Complexes **1** and **2** are suitable to test this hypothesis. The JT axis on the Mn(III) ion(s) in di-$\mu$-oxido bridged dimer complexes such as $\mathbf{1}^+$, $\mathbf{1}^0$, $\mathbf{2}^+$, or $\mathbf{2}^0$ will normally be placed perpendicular to the Mn-($\mu$-O)$_2$-Mn plane since the oxido-ligands are relatively strong ligands with both $\sigma$- and $\pi$-donation to the metal center. The elongation of one axis around the Mn(III) ion is observed in the X-ray structure of $\mathbf{2}^+$ (see above). This means that the carboxylate donor on the Mn(III) ion is located along the JT axis in $\mathbf{1}^+$ and $\mathbf{1}^0$ but not in $\mathbf{2}^+$ and $\mathbf{2}^0$. Our results indicate that a monodentate carboxylate ligand anywhere in the coordination sphere is influenced by a change in oxidation state of the Mn ion. Thus, an observed shift of a (monodentate) carboxylate stretching frequency does not require the elimination of a JT axis.

The results presented here are most relevant to the single oxidation in the $S_1 \rightarrow S_2$ transition in the S-cycle in PSII, as no charge compensation is involved. For this transition, a change in a $\nu_s$(COO) stretch from the backbone carboxylate of the C-terminal Ala344 residue on the D1 protein has been observed with FTIR spectroscopy.[23] The shift, from 1354 cm$^{-1}$ to 1338 or 1320 cm$^{-1}$ (1338 or 1320 cm$^{-1}$ to 1307 cm$^{-1}$ in a $^{13}$C-labeled sample), was attributed to increased charge or an elimination of a JT distortion on the Mn ion where Ala344 is coordinated. In the $S_3 \rightarrow S_0$ transition, this shift was restored. In the very recent 1.9 Å resolution crystal structure,[6] this residue is bridging the Mn ion labeled $Mn_2$ and the Ca ion in the WOC. However, it is an unsymmetrical bridge with a Mn–O distance of 2.0 Å and a Ca–O distance of 2.5 Å.

A downfield shift of 16–34 cm$^{-1}$ of the symmetrical stretching vibration of Ala344 is matching (the reverse of) what was observed for the two different carboxylates in the $Mn_2^{III,IV}$ to $Mn_2^{III,III}$ transition for **2** (16 and 39 cm$^{-1}$) and also match one of the bands from the carboxylates for the same reduction of **1** (22 cm$^{-1}$). The positions of the peaks from Ala344 are also closely matching the peaks observed in the difference spectra from the $\mathbf{1}^+ \rightarrow \mathbf{1}^0$ and $\mathbf{2}^+ \rightarrow \mathbf{2}^0$ transitions. For the $Mn_2^{IV,IV} \rightarrow Mn_2^{III,IV}$ transition, the shifts we observe are all somewhat larger than the shifts observed for Ala344 in the $S_1 \rightarrow S_2$ transition. Seemingly, our results show that the observed shift of the COO-stretch of Ala344 is attributable to an oxidation of either the Mn ion to which Ala344 is coordinated or, contrary to previous assignments, the neighboring Mn ion if the two ions are electronically coupled. Also, it is not required that the carboxylate is coordinated along a JT axis that is eliminated during the oxidation as previously suggested.[10]

The $S_0 \rightarrow S_1$ and $S_2 \rightarrow S_3$ transitions involve both an electron transfer and a proton release leaving the WOC with unchanged charge for either transition. It would be very informative to study high-valent Mn complexes where a similar situation is reproduced. We will pursue the investigation of a protonated $Mn_2^{III,IV}$ complex, either $H\mathbf{1}^{2+}$ or $H\mathbf{2}^{2+}$, to be able to compare the IR-stretching frequencies with $\mathbf{1}^{2+}$ or $\mathbf{2}^{2+}$ to model a one electron/one proton oxidation step.

In conclusion, our study on **1** and **2** indicate that for monodentate carboxylates, significant changes in the IR stretching frequencies can be expected for any position in the coordination sphere of a Mn ion that changes oxidation state and there is a trend of a decreasing Δ value with decreasing oxidation states. Also, in comparison with the WOC in PSII, FTIR data alone cannot ascertain which of the four Mn ions in the WOC that is oxidized.

## ■ ASSOCIATED CONTENT

### Ⓢ Supporting Information

Cyclic voltammograms of **1** and **2**, IR spectra of $\mathbf{1}(ClO_4)_2$ and $\mathbf{2}PF_6$ in KBr pellets, IR spectra of **1*** and **2***, and time-dependent spectra of oxidation and reduction to and from the $\mathbf{2}^+$ state. This material is available free of charge via the Internet at http://pubs.acs.org.

## ■ AUTHOR INFORMATION


### Corresponding Author

*E-mail: anders.thapper@fotomol.uu.se.

### Present Address

[†]Laboratoire de Chimie et Biologie des Métaux, UMR5249 CNRS-CEA-UJF, CEA Grenoble, 17 rue des Martyrs, 38054 Grenoble, Cedex 9, France.


## ■ ACKNOWLEDGMENTS

This work was supported by the Swedish Energy Agency, Knut and Alice Wallenberg Foundation, and the EU/Energy Network project SOLAR-H2 (FP7 contract no. 212508).

## ■ REFERENCES


(1) Debus, R. J. *Coord. Chem. Rev.* **2008**, *252*, 244–258.

(2) Abreu, I. A.; Cabelli, D. E. *Biochim. Biophys. Acta, Proteins Proteomics* **2010**, *1804*, 263–274.

(3) Dismukes, G. C. *Chem. Rev.* **1996**, *96*, 2909–2926.

(4) (a) Wu, A. J.; Penner-Hahn, J. E.; Pecoraro, V. L. *Chem. Rev.* **2004**, *104*, 903–938. (b) de Boer, J. W.; Browne, W. R.; Feringa, B. L.; Hage, R. *C. R. Chim.* **2007**, *10*, 341–354.

(5) Dau, H.; Haumann, M. *Coord. Chem. Rev.* **2008**, *252*, 273−295.
(6) Umena, Y.; Kawakami, K.; Shen, J.-R.; Kamiya, N. *Nature* **2011**, *473*, 55−60.
(7) (a) Wieghardt, K.; Bossek, U.; Ventur, D.; Weiss, J. *J. Chem. Soc., Chem. Commun.* **1985**, 347−349. (b) Wieghardt, K.; Bossek, U.; Nuber, B.; Weiss, J.; Bonvoisin, J.; Corbella, M.; Vitols, S. E.; Girerd, J. J. *J. Am. Chem. Soc.* **1988**, *110*, 7398−7411.
(8) Eilers, G.; Zettersten, C.; Nyholm, L.; Hammarström, L.; Lomoth, R. *Dalton Trans.* **2005**, 1033−1041.
(9) Matsushita, T.; Spencer, L.; Sawyer, D. T. *Inorg. Chem.* **1988**, *27*, 1167−1173.
(10) (a) Sproviero, E. M.; Gascón, J. A.; McEvoy, J. P.; Brudvig, G. W.; Batista, V. S. *J. Am. Chem. Soc.* **2008**, *130*, 3428−3442. (b) Sproviero, E. M.; Gascón, J. A.; McEvoy, J. P.; Brudvig, G. W.; Batista, V. S. *Coord. Chem. Rev.* **2008**, *252*, 395−415.
(11) Berggren, G.; Thapper, A.; Huang, P.; Eriksson, L.; Styring, S.; Anderlund, M. F. *Inorg. Chem.* **2011**, *50*, 3425−3430.
(12) Suzuki, M.; Senda, H.; Kobayashi, Y.; Oshio, H.; Uehara, A. *Chem. Lett.* **1988**, 1763−1766.
(13) Berggren, G.; Thapper, A.; Huang, P.; Kurz, P.; Eriksson, L.; Styring, S.; Anderlund, M. F. *Dalton Trans.* **2009**, 10044−10054.
(14) Dubois, L.; Pécaut, J.; Charlot, M.-F.; Baffert, C.; Collomb, M.-N.; Deronzier, A.; Latour, J.-M. *Chem.—Eur. J.* **2008**, *14*, 3013−3025.
(15) For monodentate carboxylates, $\nu_a$(COO) and $\nu_s$(COO) are sometimes referred to as $\nu$(C═O) (free) and $\nu$(C−O) (coordinated), respectively.
(16) The observed stretching frequencies are in the far end of what has been reported previously for metal coordinated monodentate carboxylate ligands. However, the values discussed in the literature are generally obtained from acetate and benzoate ligands. As the carboxylates in this study are covalently bound to amino-groups, which in turn are coordinated to high valent metal ions, they are relatively electron poor. This will result in shifts towards more extreme values, c.f., $CF_3COOH$ ligands in ref 17.
(17) (a) Nakamoto, K. *Infrared and Raman Spectra of Inorganic and Coordination Compounds*; John Wiley & Sons, Inc.: New York, 2008. (b) Deacon, G. B.; Phillips, R. J. *Coord. Chem. Rev.* **1980**, *33*, 227−250.
(18) The Δ values of complex **1** and **2** are always much larger than the Δ value for ionic carboxylates (e.g., Δ for ionic acetate is 164 $cm^{-1}$) as expected for monodentate carboxylates. Thus, no rearrangement of the carboxylate ligand occurs upon reduction and/or oxidation of the complexes.
(19) (a) Baffert, C.; Collomb, M.-N.; Deronzier, A.; Pécaut, J.; Limburg, J.; Crabtree, R. H.; Brudvig, G. W. *Inorg. Chem.* **2002**, *41*, 1404−1411. (b) Bian, G.-Q.; Kuroda-Sowa, T.; Konaka, H.; Maekawa, M.; Munakata, M. *Acta Crystallogr., Sect. C: Cryst. Struct. Commun.* **2004**, *60*, m338−m340. (c) Blay, G.; Fernández, I.; Pedro, J. R.; Ruiz-García, R.; Temporal-Sánchez, T.; Pardo, E.; Lloret, F.; Muñoz, M. C. *J. Mol. Catal. A: Chem.* **2006**, *250*, 20−26. (d) Ruiz-García, R.; Pardo, E.; Muñoz, M. C.; Cano, J. *Inorg. Chim. Acta* **2007**, *360*, 221−232.
(20) (a) Libby, E.; Webb, R. J.; Streib, W. E.; Folting, K.; Huffman, J. C.; Hendrickson, D. N.; Christou, G. *Inorg. Chem.* **1989**, *28*, 4037−4040. (b) Huang, D.; Wang, W.; Zhang, X.; Chen, C.; Chen, F.; Liu, Q.; Liao, D.; Li, L.; Sun, L. *Eur. J. Inorg. Chem.* **2004**, *2004*, 1454−1464.
(21) Octahedral high-spin manganese(III) ions are subject to a Jahn−Teller distortion, which usually results in an elongation along one axis in the coordination sphere of the manganese ion.[22]
(22) Greenwood, N. N.; Earnshaw, A. *Chemistry of the Elements*, 2nd ed.; Elsevier: New York, 1998.
(23) (a) Chu, H.-A.; Hillier, W.; Debus, R. J. *Biochemistry* **2004**, *43*, 3152−3166. (b) Kimura, Y.; Mizusawa, N.; Yamanari, T.; Ishii, A.; Ono, T.-A. *J. Biol. Chem.* **2005**, *280*, 2078−2083.